



1 **UV and Infrared Absorption Spectra, Atmospheric Lifetimes, and Ozone Depletion and**  
2 **Global Warming Potentials for CCl<sub>2</sub>FCCl<sub>2</sub>F (CFC-112), CCl<sub>3</sub>CClF<sub>2</sub> (CFC-112a), CCl<sub>3</sub>CF<sub>3</sub>**  
3 **(CFC-113a), and CCl<sub>2</sub>FCF<sub>3</sub> (CFC-114a)**

4 Maxine E. Davis,<sup>1,2,3</sup> François Bernard,<sup>1,2</sup> Max R. McGillen,<sup>1,2</sup>  
5 Eric L. Fleming,<sup>4,5</sup> and James B. Burkholder<sup>1</sup>

6 <sup>1</sup> Earth System Research Laboratory, Chemical Sciences Division, National Oceanic and  
7 Atmospheric Administration, Boulder, Colorado, USA.

8 <sup>2</sup> Cooperative Institute for Research in Environmental Sciences, University of Colorado,  
9 Boulder, Colorado, USA.

10 <sup>3</sup> Michigan State University, Lyman Briggs College, East Lansing, MI.

11 <sup>4</sup> NASA Goddard Space Flight Center, Greenbelt, Maryland, USA.

12 <sup>5</sup> Science Systems and Applications, Inc., Lanham, Maryland, USA.

13

14

15

16 Corresponding author: James B. Burkholder, NOAA, 325 Broadway, Boulder, CO 80305, USA.

17 ([James.B.Burkholder@noaa.gov](mailto:James.B.Burkholder@noaa.gov))

18

19

20

21

22



23 **Abstract** The potential impact of the recently observed  $\text{CCl}_2\text{FCCl}_2\text{F}$  (CFC-112),  $\text{CCl}_3\text{CClF}_2$   
24 (CFC-112a),  $\text{CCl}_3\text{CF}_3$  (CFC-113a), and  $\text{CCl}_2\text{FCF}_3$  (CFC-114a) (chlorofluorocarbons, CFCs), on  
25 stratospheric ozone and climate are presently not well characterized. In this study, the UV  
26 absorption spectra of these CFCs were measured between 192.5–235 nm over the temperature  
27 range 207–323 K. Precise parameterizations of the UV absorption spectra are presented. A 2-D  
28 atmospheric model was used to evaluate the CFC atmospheric loss processes, lifetimes, ozone  
29 depletion potentials (ODPs), and the associated uncertainty ranges in these metrics. The CFCs  
30 are primarily removed in the stratosphere by short wavelength UV photolysis with calculated  
31 global annually averaged steady-state lifetimes (years) of 63.6 (61.9–64.7), 51.5 (50.0–52.6),  
32 55.4 (54.3–56.3), and 105.3 (102.9–107.4) for CFC-112, CFC-112a, CFC-113a, and CFC-114a,  
33 respectively. The range of lifetimes given in parentheses were obtained by including the  $2\sigma$   
34 uncertainty in the UV absorption spectra and  $\text{O}(^1\text{D})$  rate coefficients in the model calculations.  
35 The 2-D model was also used to calculate the CFC ozone depletion potentials (ODPs) with  
36 values of 0.98, 0.86, 0.73, and 0.72 obtained for CFC-112, CFC-112a, CFC-113a, and CFC-  
37 114a, respectively. Using the infrared absorption spectra and lifetimes determined in this work,  
38 the CFCs global warming potentials (GWPs) were estimated to be 4260 (CFC-112), 3330 (CFC-  
39 112a), 3650 (CFC-113a), and 6510 (CFC-114a) for the 100-year time-horizon.

40

41

42



## 43 1. Introduction

44 Chlorofluorocarbons (CFCs) are potent ozone depleting and greenhouse gases that were  
45 phased-out of production under the Montreal Protocol Agreement (1987) and its subsequent  
46 amendments and adjustments. Laube et al. (2014) recently reported the first observation of  
47 tetrachloro-1,2-difluoroethane ( $\text{CCl}_2\text{FCCl}_2\text{F}$ , CFC-112), tetrachloro-1,1-difluoroethane  
48 ( $\text{CCl}_3\text{CClF}_2$ , CFC-112a), and 1,1,1-trichloro-2,2,2-trifluoroethane ( $\text{CCl}_3\text{CF}_3$ , CFC-113a) in the  
49 atmosphere with emission sources dating back to the 1960s. The atmospheric loading in the year  
50 2000 were found to be  $\sim 0.5$  ppt (CFC-112),  $\sim 0.08$  ppt (CFC-112a), and  $\sim 0.3$  ppt (CFC-113a),  
51 which are minor compared to a total chlorine loading of 3.3 ppb (year 2012), where  $\text{CCl}_3\text{F}$  (CFC-  
52 11),  $\text{CCl}_2\text{F}_2$  (CFC-12), and  $\text{CCl}_2\text{FCClF}_2$  (CFC-113) account for  $\sim 60\%$  of the total (WMO, 2014).  
53 The atmospheric abundance of CFC-112 and CFC-112a was found to have leveled off in the late  
54 1990's, while the abundance of CFC-113a was found to be increasing through to the present day,  
55 which is contrary to the objectives of the Montreal Protocol. Laube et al. (2014) estimated the  
56 stratospheric lifetimes for these substances, using a tracer-tracer analysis, to be 51 (37–82), 44  
57 (28–98), and 51 (27–264) years for CFC-112, CFC-112a, and CFC-113a, respectively, where the  
58 values in parentheses are the range of the lifetimes determined in their analysis. The inferred  
59 ozone depletion potentials (ODPs) were 0.88 (0.62–1.44), 0.88 (0.5–2.19), and 0.68 (0.34–3.79)  
60 for CFC-112, CFC-112a, and CFC-113a, respectively, where the range in parentheses was  
61 derived from the range in the CFC lifetime given above. It is clear that the CFCs are long-lived  
62 compounds and potent ozone depleting substances and greenhouse gases. It is expected that  
63 these compounds would be predominantly removed from the atmosphere via short wavelength  
64 UV photolysis, primarily in the stratosphere. However, to date, there are no UV absorption  
65 spectra for these compounds available, which are needed to better evaluate their atmospheric  
66 impact.

67 In this study, UV absorption spectra were measured for CFC-112, CFC-112a, CFC-113a,  
68 and 1,1-dichlorotetrafluoroethane ( $\text{CCl}_2\text{FCF}_3$ , CFC-114a) between 192.5 and 235 nm over the  
69 temperature range 207–323 K. The Goddard Space Flight Center (GSFC) 2-D atmospheric  
70 model was used to evaluate the reactive and photolytic loss processes and calculate globally  
71 averaged lifetimes and ozone depletion potentials. In addition, infrared absorption spectra were  
72 measured at 296 K for these compounds and used to estimate their global warming potentials



73 (GWPs). The present results are compared with results from the previous infrared studies of  
74 Olliff and Fischer (1992; 1994) and Etminan et al. (2014) where possible.

## 75 2. Experimental Details

### 76 2.1 UV Measurements

77 The experimental apparatus has been described in detail previously (McGillen et al.,  
78 2013; Papadimitriou et al., 2013a; 2013b) and is only briefly discussed here. The output of a  
79 stable 30 W deuterium (D<sub>2</sub>) lamp light source was collimated and directed through a jacketed  
80 90.4 ± 0.3 cm single pass absorption cell. The beam exiting the cell was focused onto the  
81 entrance slit (150 μm) of a 0.25 m monochromator and detected using a photomultiplier tube  
82 (PMT). The temperature of the absorption cell was controlled to within ±1 K. Absorption  
83 measurements were made at 10 discrete wavelengths at temperatures between 207 and 323 K.

84 Beer's law was applied to determine the absorption cross section,  $\sigma(\lambda, T)$ , at each  
85 wavelength and temperature:

$$86 \quad A(\lambda, T) = \ln \left[ \frac{I_0(\lambda) - I_d}{I(\lambda) - I_d} \right] = \sigma(\lambda, T) \times L \times [\text{CFC}] \quad (1)$$

87 where  $A(\lambda, T)$  is the absorbance at wavelength  $\lambda$  and temperature  $T$ ,  $I_d$  is the signal recorded in  
88 the absence of light,  $I_0(\lambda)$  and  $I(\lambda)$  are the measured signal in the absence and presence of the  
89 CFC sample,  $L$  is the cell pathlength, and [CFC] is the gas-phase CFC concentration. The PMT  
90 signal was recorded with a 1 kHz sampling rate and a ~20 s average was used in the data  
91 analysis.  $I_0(\lambda)$  was recorded at the beginning and end of each measurement, which typically  
92 agreed to 0.1%, or better. Absorbance measurements were made at each wavelength over a  
93 range of CFC concentration under static conditions. The CFCs were added to the absorption cell  
94 from dilute mixtures and the CFC concentration was determined using the sample mixing ratio,  
95 the absorption cell pressure and temperature, and the ideal gas law. A linear least-squares fit of  
96  $A(\lambda, T)$  versus [CFC] was used to obtain  $\sigma(\lambda, T)$ .

97 For the CFC-112 and CFC-112a measurements, an optical neutral density filter was  
98 inserted between the D<sub>2</sub> lamp and the absorption cell to attenuate the probe beam and minimize  
99 CFC loss due to photolysis (sample photolysis was not observed for CFC-113a and CFC-114a).  
100 In addition, a mechanical shutter blocked the D<sub>2</sub> lamp beam while the absorption cell was being  
101 filled. Under most conditions, photolytic loss of the CFC-112 and CFC-112a was undetectable.  
102 However, at the higher concentrations used in this study minor photolytic loss (<2%) was



103 observed. In these cases, a least-squares fit of the first ~20 s of the PMT signal was used in the  
104 data analysis to obtain the initial  $I(\lambda)$  signal.

## 105 2.2 Infrared Absorption Measurements

106 Infrared absorption spectra at 296 K for CFC-112, CFC-112a, CFC-113a, and CFC-114a  
107 were measured over the 500 to 4000  $\text{cm}^{-1}$  wavenumber range using Fourier transform infrared  
108 (FTIR) spectroscopy. Measurements were made using a 15 cm single pass absorption cell at a  
109 resolution of 1  $\text{cm}^{-1}$  with 100 co-adds. The CFC sample was introduced into the absorption cell  
110 from a dilute mixture prepared off-line and the CFC concentration was determined using the  
111 ideal gas law. Absorption cross sections were determined using Beer's law, Eq. (1), with the  
112 spectrum measurements consisting of ~10 different concentrations. The concentration ranges  
113 used were (in  $10^{16}$  molecule  $\text{cm}^{-3}$ ): (0.348–10.2), (0.453–3.84), (0.376–1.90), and (0.279–4.02)  
114 for CFC-112, CFC-112a, CFC-113a, and CFC-114a, respectively. The infrared absorption  
115 spectra recorded for CFC-112 and CFC-112a were corrected for the presence of a minor (~4%)  
116 isomer impurity as determined from a  $^{19}\text{F}$  NMR sample analysis.

## 117 2.3 Materials

118 Samples of  $\text{CCl}_2\text{FCCl}_2\text{F}$  (CFC-112, 97% stated purity),  $\text{CCl}_3\text{CClF}_2$  (CFC-112a, 96%  
119 stated purity),  $\text{CCl}_3\text{CF}_3$  (CFC-113a, 99% stated purity), and  $\text{CCl}_2\text{FCF}_3$  (CFC-114a, 99.9% stated  
120 purity) were obtained commercially. The samples were processed in several freeze (77 K)-  
121 pump-thaw cycles prior to use. The CFC-114a sample was also treated with freeze (197 K)-  
122 pump-thaw cycles to remove  $\text{CO}_2$  from the sample. The liquid CFC-112, CFC-112a, and CFC-  
123 113a samples were stored under vacuum in Pyrex reservoirs. The CFC-112 and CFC-112a  
124 samples contained minor isomeric impurities, which were quantified using  $^{19}\text{F}$  NMR to be  
125 0.960/0.040 (CFC-112a/CFC-112) for the CFC-112a sample and 0.963/0.0368 (CFC-112/CFC-  
126 112a) for the CFC-112 sample. Dilute mixtures of the CFCs in a He (UHP, 99.999%) bath gas  
127 were prepared manometrically in 12 L Pyrex bulbs and used to deliver the CFC sample to the  
128 UV and infrared absorption cells. Over the course of the study, multiple gas mixtures were  
129 prepared for each of the CFCs with mixing ratios ranging between 0.5 and 27%. The dilute  
130 mixtures were prepared with an estimated accuracy of  $\pm\sim 1\%$ . The UV and infrared spectra  
131 obtained for the CFCs were independent of the sample mixing ratio and absorption cell total  
132 pressure. Pressures were measured using calibrated capacitance manometers. Uncertainties  
133 given throughout the paper are  $2\sigma$  unless noted otherwise.



134 **3. Results and Discussion**

135 The absorption spectrum,  $\sigma(\lambda, T)$ , measurements obeyed Beer's law with fit precisions of  
136 ~1%, or less, for all wavelengths and temperatures included in this study. Replicate  
137 measurements using different sample mixing ratios, bath gas, range of absorption, and optical  
138 filtering agreed to within the measurement precision and were combined in a global linear least-  
139 squares fit in the final data analysis.

140 The UV absorption spectra of the CFC-112 and CFC-112a samples were measured at 10  
141 discrete wavelengths between 192.5 nm and 235 nm at 5 discrete temperatures between 230 and  
142 323 K. The results, not corrected for the isomeric impurity present in the samples, are  
143 summarized in Tables S1 and S2 and shown in Figures S1 and S2 of the Supporting Information.  
144 To account for the isomeric impurity,  $\sigma(\lambda, T)$  for CFC-112 and CFC-112a were parameterized  
145 using the empirical formula:

$$146 \quad \ln(\sigma(\lambda, T)) = \sum_i A_i \lambda_i^i + (T - 296) \sum_i B_i \lambda_i^i \quad (2)$$

147 The parameterizations reproduced the experimental data to better than ~2% over the wavelength  
148 range most critical to atmospheric photolysis, i.e., between 195 and 215 nm. The results from  
149 the  $^{19}\text{F}$  NMR sample analysis were then used to obtain the final spectrum parameterizations.

150 The UV absorption spectra for CFC-113a and CFC-114a were measured at 10 discrete  
151 wavelengths between 192.5 and 235 nm at 6 discrete temperatures between 207 and 323 K. The  
152 cross section results are given in Tables 1 and 2 and shown in Figures 1 and 2. The CFC UV  
153 absorption spectra were parameterized using Eq. (2). The parameterizations reproduced the  
154 experimental data to within ~4%, or better, as shown in Figures 1 and 2.

155 The fit parameters are given in Table 3 and a comparison of the parameterized 296 K  
156 spectra is shown in Figure 3. The UV absorption spectra of the CFCs are continuous over the  
157 wavelength range included in this study with a precipitous decrease in cross section with  
158 increasing wavelength. A decrease in  $\sigma(\lambda, T)$  with decreasing temperature was observed at  
159 nearly all wavelengths included in this study with the temperature dependence being greatest at  
160 the longer wavelengths, see Figures 1, 2, and S1 and S2. The inclusion of the  $\sigma(\lambda, 323 \text{ K})$   
161 measurements, although not entirely atmospherically relevant, was included in the study to better  
162 define the absorption spectrum temperature dependence and its parameterization. As shown in  
163 Figure 3, the UV absorption spectra for the CFCs show distinct differences in their absolute cross  
164 sections and wavelength dependence over the region most critical for determining their



165 atmospheric photolysis rates, i.e., lifetimes. The spectra demonstrate that CFCs with increased  
166 chlorine content are stronger absorbers in this wavelength region, although the molecular  
167 structure of the molecule also plays an important role. For example, the  $C_2Cl_4F_2$  isomer with  
168 more chlorine atoms on a carbon atom, CFC-112a ( $CCl_3CClF_2$ ), absorbs more strongly than  
169 CFC-112 ( $CCl_2FCCl_2F$ ).

170 The spectrum parameterizations given in Table 3 reproduce the experimental data very  
171 well. The overall  $2\sigma$  uncertainty in  $\sigma(\lambda, T)$  for CFC-112, CFC-112a, CFC-113, and CFC-114a,  
172 including estimated systematic errors, is estimated to be  $\sim 4\%$  over the range of wavelengths and  
173 temperatures included in this study.

174 The measured infrared spectra for each of the CFCs obeyed Beer's law with a fit  
175 precision of  $\sim 0.3\%$  and were independent of total pressure over the pressure range 20–250 Torr  
176 (He bath gas). The infrared spectra are shown in Figure 4 and digitized spectra are available in  
177 the Supporting Information. Table S3 in the Supporting Information provides a detailed  
178 comparison of our results with those of Olliff and Fischer (1992; 1994) for all the CFCs and  
179 Etminan et al. (2014) for CFC-113a. Overall the agreement between the studies is better than  
180 10%.

#### 181 4. Atmospheric Implications

182 The atmospheric loss processes, lifetimes, ODPs, and associated uncertainties for the  
183 CFCs included in this study were quantified using the Goddard Space Flight Center (GSFC) 2-D  
184 atmospheric model (Fleming et al., 2011). The calculations used the UV spectrum  
185 parameterizations obtained in this work with an assumed unit photolysis quantum yield at all  
186 wavelengths. As discussed in section 3, an overall  $2\sigma$  uncertainty of 4% was used at all  
187 wavelengths and temperatures for the UV cross sections of the four CFCs. For Lyman-  
188  $\alpha$  (121.567 nm), absorption cross sections are not available for these CFCs and values (in units  
189 of  $10^{-17} \text{ cm}^2 \text{ molecule}^{-1}$ ) of 13, 15, 9.8, and 2 were estimated for CFC-112, CFC-112a, CFC-  
190 113a, and CFC-114a, respectively, based on values available for similar molecules (see Ko et al.  
191 (2013), Chapter 3). An estimated Lyman- $\alpha$  cross section uncertainty factor of 2 ( $2\sigma$ ) was used.  
192 Rate coefficients for the  $O(^1D)$  reaction with CFC-113a and CFC-114a were taken from  
193 Baasandorj et al. (2011) with  $2\sigma$  uncertainty factors of 1.25 and 1.2, respectively. Rate  
194 coefficients for the  $O(^1D)$  reaction with CFC-112 and CFC-112a were estimated to be  $3 \times 10^{-10}$



195  $\text{cm}^3 \text{ molecule}^{-1} \text{ s}^{-1}$  with a 0.9 reactive branching ratio and an uncertainty factor of 1.5 ( $2\sigma$ ). All  
196 other kinetic and photochemical parameters were taken from Sander et al. (2011). All model  
197 results presented in this study are for year 2000 steady-state conditions.

198 Model calculations of the CFC fractional atmospheric loss processes are given in Table 4  
199 and the altitude profiles for CFC-112 are shown in Figure 5. The calculated atmospheric profiles  
200 for CFC-112a, CFC-113a, and CFC-114a are provided in the Supporting Information. UV  
201 photolysis is the predominant atmospheric loss process for each of the CFCs. Lyman- $\alpha$   
202 photolysis is important only in the mesosphere above 65 km; it has a negligible contribution to  
203 the overall global loss ( $<0.001$ ). The  $\text{O}(^1\text{D})$  reaction is a minor stratospheric loss process,  $\sim 2\%$ ,  
204 for CFC-112, CFC-112, and CFC-113a, but more significant for CFC-114a,  $\sim 7\%$ . The UV  
205 photolysis and  $\text{O}(^1\text{D})$  reactive loss of the CFCs leads to the direct release of reactive chlorine and  
206 the formation of chlorine containing radicals (Burkholder et al., 2015).

207 The CFC lifetimes were computed as the ratio of the annually averaged global  
208 atmospheric burden to the vertically integrated annually averaged total global loss rate (Ko et al.,  
209 2013). The total global lifetime ( $\tau_{\text{Tot}}$ ) was also separated by the troposphere ( $\tau_{\text{Trop}}$ , surface to the  
210 tropopause, seasonally and latitude-dependent), stratosphere ( $\tau_{\text{Strat}}$ ), and mesosphere ( $\tau_{\text{Meso}}$ ,  $<1$   
211 hPa) using the total global atmospheric burden and the loss rate integrated over the different  
212 atmospheric regions such that

$$213 \quad \frac{1}{\tau_{\text{Tot}}} = \frac{1}{\tau_{\text{Trop}}} + \frac{1}{\tau_{\text{Strat}}} + \frac{1}{\tau_{\text{Meso}}} \quad (2)$$

214 The 2-D model total global annually averaged lifetimes and the range in lifetimes are given in  
215 Table 5. The  $2\sigma$  range in the lifetime was calculated using the absolute  $2\sigma$  maximum and  
216 minimum in the UV absorption spectra and estimated Lyman- $\alpha$  cross sections reported in the  
217 present work, along with the  $2\sigma$  uncertainties in the  $\text{O}(^1\text{D})$  rate coefficients taken from Sander et  
218 al. (2011). The CFCs are long-lived and primarily removed in the stratosphere by UV  
219 photolysis. The uncertainty in the calculated lifetime due to the uncertainty in the UV absorption  
220 spectra measured in this work is small,  $<2\%$ . The absolute lifetime uncertainty due to the kinetic  
221 and photochemical input parameters is expected to be small compared to that calculated using  
222 different atmospheric models due to the individual model treatment of dynamics, chemistry,  
223 radiation, numeric, and other processes (Chipperfield et al., 2014; Ko et al., 2013).



224 The model calculated stratospheric lifetimes for CFC-112, CFC-112a, and CFC-113a are  
225 in reasonable agreement with the values of 51 (37–82), 44 (28–98), and 51 (27–264) years  
226 reported by Laube et al. (2014) (uncertainty ranges in parentheses). The lifetimes reported by  
227 Laube et al. were based on a tracer-tracer analysis (see Plumb and Ko (1992) and Volk et al.  
228 (1997) for method details) using a reference CFC-11 lifetime of 45 years. Scaling to the 52 year  
229 CFC-11 lifetime given in WMO (2014) brings the results into better agreement with the present  
230 work. The range of lifetimes obtained in the model results, which was determined solely based  
231 on the uncertainty in the kinetic and photochemical input parameters, is, however, significantly  
232 less than obtained in the tracer-tracer analysis. It is worth noting that while the total global  
233 lifetimes of the isomers CFC-112 and CFC-112a are similar, the lifetimes of CFC-113a (55.4  
234 yrs) and CFC-114a (105.3 yrs) are substantially shorter (by ~60%) than those of the isomers  
235 CFC-113 (93 yrs) and CFC-114 (189 yrs) (WMO, 2014).

#### 236 4.1. Ozone Depletion Potentials (ODPs)

237 The semi-empirical and model calculated ODPs for the CFCs are given in Table 6. The  
238 ODP was calculated following the methodology used previously (Fisher et al., 1990; Wuebbles,  
239 1983). Steady-state simulations for year 2000 were run with the surface boundary conditions for  
240 the four CFCs and CFC-11 (used as the reference compound) increased individually to obtain a  
241 ~1% depletion in annually averaged global total ozone. The ODP was then taken as the change  
242 in global ozone per unit mass emission of the CFC relative to the change in global ozone per unit  
243 mass emission of CFC-11. Each of these compounds is a potent ozone depleting substance. The  
244 model calculated ODPs for CFC-112, CFC-112a, and CFC-113a are similar to the semi-  
245 empirical values inferred by Laube et al. (2014). The small range ( $\leq \pm 0.015$ ) in the model ODP  
246 values is primarily due to the relatively small uncertainty in the UV spectra obtained in this  
247 work.

248 Table 6 also includes ODPs for CFC-113 and CFC-114. These are larger than the ODPs  
249 for the isomers CFC-113a and CFC-114a (especially CFC-113 vs CFC-113a), likely due in part,  
250 to the longer lifetimes of CFC-113 and CFC-114. For comparison with other related compounds,  
251 the ODPs of CFC-115, CFC-12, and  $\text{CCl}_4$  are also included in Table 6. This shows the general  
252 decrease in ODP with decreasing chlorination among CFC-112a, CFC-112, CFC-113a, CFC-  
253 113, CFC-114a, CFC-114, and CFC-115. We also note that the model ODPs for CFC-112 and  
254 CFC-112a are generally similar, although slightly less, than  $\text{CCl}_4$  which also contains 4 chlorine



255 atoms. For most of the compounds listed in Table 6, the model ODPs are larger than the semi-  
256 empirical values, likely due in part, to differences in the observationally based fractional release  
257 factors compared to the model calculations.

#### 258 **4.2. Calculated Radiative Efficiencies (RE) and Global Warming Potentials (GWPs)**

259 Table 6 summarizes the radiative efficiencies (REs) for the CFCs calculated using the  
260 methods described in Hodnebrog et al. (2013) and the global warming potentials (GWPs) for the  
261 20, 100, and 500-year time-horizons using the lifetimes from this work. The CFCs are potent  
262 greenhouse gases and radiative forcing agents due to their high REs and long atmospheric  
263 lifetimes. The GWPs for these long-lived compounds are comparable, or less than, those of the  
264 atmospherically most abundant CFCs, e.g. the 100 year time-horizon GWPs for CFC-11 ( $\text{CCl}_3\text{F}$ ),  
265 CFC-12 ( $\text{CCl}_2\text{F}_2$ ), and CFC-113 ( $\text{CCl}_2\text{FCClF}_2$ ) are 4660, 10200, and 5820, respectively (WMO,  
266 2014).

#### 267 **5. Conclusions**

268 Short wavelength UV absorption spectra for  $\text{CCl}_2\text{FCCl}_2\text{F}$  (CFC-112),  $\text{CCl}_3\text{CClF}_2$  (CFC-  
269 112a),  $\text{CCl}_3\text{CF}_3$  (CFC-113a), and  $\text{CCl}_2\text{FCF}_3$  (CFC-114a) measured in this work between 192.5  
270 and 235 nm and at temperatures in the range 207 to 323 K were combined with 2-D atmospheric  
271 model calculations to assess their atmospheric loss processes, lifetimes, and ozone depletion  
272 potentials (ODPs). Short wavelength UV photolysis was shown to be the predominant loss  
273 process for the CFCs with global annually averaged lifetimes of 63.6, 51.5, 55.5, and 105.3  
274 years, for CFC-112, CFC-112a, CFC-113a, and CFC-114a, respectively. The uncertainty in the  
275 model-calculated lifetimes due primarily to the  $2\sigma$  uncertainty in the UV absorption spectra  
276 reported in this work, was found to be small,  $<3\%$ . These CFCs are potent ozone depleting  
277 substances with 2-D model calculated ODPs of 0.98, 0.86, 0.73, and 0.72 for CFC-112, CFC-  
278 112a, CFC-113a, and CFC-114a, respectively. The uncertainty in the model calculated ODPs  
279 due to the uncertainty in the UV spectra and  $\text{O}(^1\text{D})$  reactive loss is small,  $\leq \pm 0.015$ . These CFCs  
280 are also potent greenhouse gases with GWPs comparable to those of the most abundant CFCs  
281 present in the atmosphere.

282 **Acknowledgments.** This work was supported in part by NOAA's Atmospheric Chemistry,  
283 Carbon Cycle, and Climate (AC4) Program and NASA's Atmospheric Composition Program.  
284 Supporting information includes digitized infrared spectra as well as additional figures, model  
285 results, and tables.

287 **References**

288

289 Baasandorj, M., Feierabend, K. J., and Burkholder, J. B.: Rate coefficients and ClO radical yields  
290 in the reaction of O(<sup>1</sup>D) with CClF<sub>2</sub>CCl<sub>2</sub>F, CCl<sub>3</sub>CF<sub>3</sub>, CClF<sub>2</sub>CClF<sub>2</sub>, and CCl<sub>2</sub>FCF<sub>3</sub>, *Int. J.*  
291 *Chem Kinet.*, 43, 1-9, doi:10.1002/kin.20561, 2011.

292 Burkholder, J. B., Cox, R. A., and Ravishankara, A. R.: Atmospheric degradation of ozone  
293 depleting substances, their substitutes, and related species, *Chem. Rev.*, 115, 3704-3759,  
294 doi:10.1021/cr5006759, 2015.

295 Chipperfield, M. P., Liang, Q., Strahan, S. E., Morgenstern, O., Dhomse, S. S., Abraham, N. L.,  
296 Archibald, A. T., Bekki, S., Braesicke, P., Di Genova, G., Fleming, E. L., Hardiman, S.  
297 C., Iachetti, D., Jackman, C. H., Kinnison, D. E., Marchand, M., Pitari, G., Pyle, J. A.,  
298 Rozanov, E., Stenke, A., and Tummon, F.: Multimodel estimates of atmospheric lifetimes  
299 of long-lived ozone-depleting substances: Present and future, *J. Geophys. Res.*, 119,  
300 2555–2573, doi:10.1002/2013/13JD021097, 2014.

301 Etminan, M., Highwood, E. J., Laube, J. C., McPheat, R., Marston, G., Shine, K. P., and Smith,  
302 K. M.: Infrared absorption spectra, radiative efficiencies, and global warming potentials  
303 of newly-detected halogenated compounds: CFC-113a, CFC-112 and HCFC-133a,  
304 *Atmosphere*, 5, 473-483, doi:10.3390/atmos5030473, 2014.

305 Fisher, D. A., Hales, C. H., Filkin, D. L., Ko, M. K. W., Sze, N. D., Connell, P. S., Wuebbles, D.  
306 J., Isaksen, I. S. A., and Stordal, F.: Model calculations of the relative effects of CFCs  
307 and their replacements on stratospheric ozone, *Nature*, 344, 508–512,  
308 doi:10.1038/344513a0, 1990.

309 Fleming, E. L., Jackman, C. H., Stolarski, R. S., and Douglas, A. R.: A model study of the  
310 impact of source gas changes on the stratosphere for 1850-2100, *Atmos. Chem. Phys.*,  
311 11, 8515-8541, doi:10.5194/acp-11-8515-2011, 2011.

312 Hodnebrog, Ø., Etminan, M., Fuglestvedt, J. S., Marston, G., Myhre, G., Nielsen, C. J., Shine, K.  
313 P., and Wallington, T. J.: Global warming potentials and radiative efficiencies of  
314 halocarbons and related compounds: A comprehensive review, *Rev. Geophys.*, 51, 300–  
315 378, doi:10.1002/rog.20013, 2013.

316 Ko, M. K. W., Newman, P. A., Reimann, S., Strahan, S. E., Plumb, R. A., Stolarski, R. S.,  
317 Burkholder, J. B., Mellouki, W., Engel, A., Atlas, E. L., Chipperfield, M., and Liang, Q.  
318 (eds), 2013, *Lifetimes of Stratospheric Ozone-Depleting Substances, Their*  
319 *Replacements, and Related Species*, p.

320 Laube, J. C., Newland, M. J., Hogan, C., Brenninkmeijer, C. A. M., Fraser, P. J., Martinerie, P.,  
321 Oram, D. E., Reeves, C. E., Röckmann, T., Schwander, J., Witrant, E., and Sturges, W.  
322 T.: Newly detected ozone-depleting substances in the atmosphere, *Nature Geoscience*, 7,  
323 266-269, doi:10.1038/ngeo2109, 2014.

324 McGillen, M. R., Fleming, E. L., Jackman, C. H., and Burkholder, J. B.: CFC<sub>13</sub> (CFC-11): UV  
325 absorption spectrum temperature dependence measurements and the impact on its  
326 atmospheric lifetime and uncertainty, *Geophys. Res. Lett.*, 40, 4772-4776,  
327 doi:10.1002/grl.50915, 2013.

328 Olliff, M., and Fischer, G.: Integrated band intensities of 1,1,1-trichlorotrifluoroethane,  
329 CFC113a, and 1,1,2-trichlorotrifluoroethane, CFC113, *Spectrochimica Acta Part a-*  
330 *Molecular and Biomolecular Spectroscopy*, 48, 229-235, doi:10.1016/0584-  
331 8539(92)80028-u, 1992.



- 332 Olliff, M. P., and Fischer, G.: Integrated absorption intensities of haloethanes and halopropanes,  
333 Spectrochimica Acta Part a-Molecular and Biomolecular Spectroscopy, 50, 2223-2237,  
334 doi:10.1016/0584-8539(93)e0027-t, 1994.
- 335 Papadimitriou, V. C., McGillen, M. R., Fleming, E. L., Jackman, C. H., and Burkholder, J. B.:  
336 NF<sub>3</sub>: UV absorption spectrum temperature dependence and the atmospheric and climate  
337 forcing implications, Geophys. Res. Lett., 40, 1-6, doi:10.1002/grl.50120, 2013a.
- 338 Papadimitriou, V. C., McGillen, M. R., Smith, S. C., Jubb, A. M., Portmann, R. W., Hall, B. D.,  
339 Fleming, E. L., Jackman, C. H., and Burkholder, J. B.: 1,2-Dichlorohexafluoro-  
340 cyclobutane (1,2-c-C<sub>4</sub>F<sub>6</sub>Cl<sub>2</sub>, R-316c) a potent ozone depleting substance and greenhouse  
341 gas: Atmospheric loss processes, lifetimes, and ozone depletion and global warming  
342 potentials for the (*E*) and (*Z*) stereoisomers, J. Phys. Chem. A, 117, 11049-11065,  
343 doi:10.1021/jp407823k, 2013b.
- 344 Plumb, R. A., and Ko, M. K. W.: Interrelationships between mixing ratios of long-lived  
345 stratospheric constituents, J. Geophys. Res., 97, 10140-10156, doi:10.1029/92JD00450,  
346 1992.
- 347 Sander, S. P., Abbatt, J., Barker, J. R., Burkholder, J. B., Friedl, R. R., Golden, D. M., Huie, R.  
348 E., Kolb, C. E., Kurylo, M. J., Moortgat, G. K., Orkin, V. L., and Wine, P. H.: Chemical  
349 Kinetics and Photochemical Data for Use in Atmospheric Studies, Evaluation Number  
350 17, 2011, <http://jpldataeval.jpl.nasa.gov>.
- 351 Volk, C. M., Elkins, J. W., Fahey, D. W., Dutton, D. S., Gilligan, J. M., Loewenstein, M.,  
352 Podolske, J. R., Chan, K. R., and Gunson, M. R.: Evaluation of source gas lifetimes from  
353 stratospheric observations, J. Geophys. Res., 102, 25543-25564, doi:10.1029/97JD02215,  
354 1997.
- 355 WMO (eds), 2014, WMO (World Meteorological Organization), Scientific Assessment of Ozone  
356 Depletion: 2014, Global Ozone Research and Monitoring Project-Report No. 55, p. 416  
357 pp.
- 358 Wuebbles, D. J.: Chlorocarbon emission scenarios: potential impact on stratospheric ozone,  
359 Geophys. Res. Lett., 88, 1433-1443, doi:10.1029/JC88iC02p01433, 1983.
- 360
- 361
- 362



363 **Table 1.** CCl<sub>3</sub>CF<sub>3</sub> (CFC-113a) UV Absorption Cross Section Data (10<sup>-20</sup> cm<sup>2</sup> molecule<sup>-1</sup>, base e)  
 364 Obtained in This Work.

λ (nm)	323 K	296 K	271 K	250 K	232 K	207 K
192.5	131.6 ± 1.5	132.5 ± 1.1	136.9 ± 1.0	137.2 ± 0.9	141.4 ± 1.6	139.7 ± 0.9
195	103.9 ± 0.2	106.6 ± 0.6	106.8 ± 0.9	107.5 ± 1.2	110.2 ± 1.0	111.0 ± 0.3
200	64.3 ± 0.2	63.9 ± 0.6	63.9 ± 1.2	63.6 ± 0.6	64.5 ± 0.6	63.5 ± 0.4
205	35.3 ± 0.14	34.1 ± 0.2	33.5 ± 0.13	33.2 ± 0.2	31.9 ± 0.3	31.3 ± 0.3
210	17.3 ± 0.10	16.2 ± 0.1	15.3 ± 0.1	14.4 ± 0.1	13.9 ± 0.17	12.5 ± 0.2
215	7.99 ± 0.02	7.25 ± 0.01	6.58 ± 0.02	5.94 ± 0.06	5.77 ± 0.06	5.26 ± 0.07
220	3.57 ± 0.014	3.07 ± 0.02	2.65 ± 0.007	2.36 ± 0.02	2.23 ± 0.008	2.09 ± 0.02
225	1.55 ± 0.014	1.29 ± 0.01	1.04 ± 0.004	0.912 ± 0.006	0.813 ± 0.01	0.778 ± 0.04
230	0.673 ± 0.009	0.521 ± 0.004	0.418 ± 0.003	0.357 ± 0.008	0.322 ± 0.003	
235	0.297 ± 0.018	0.208 ± 0.001	0.157 ± 0.006	0.139 ± 0.006		

365 \* Quoted uncertainties are 2σ fit precision values (rounded off).

366



367

368 **Table 2.** CCl<sub>2</sub>FCF<sub>3</sub> (CFC-114a) UV Absorption Cross Section Data (10<sup>-20</sup> cm<sup>2</sup> molecule<sup>-1</sup>, base  
369 e) Obtained in This Work.

λ (nm)	323 K	296 K	271 K	250 K	232 K	207 K
192.5	32.8 ± 0.2	32.2 ± 0.3	31.6 ± 0.2	30.7 ± 0.2	30.0 ± 0.3	28.2 ± 0.2
195	21.8 ± 0.1	20.7 ± 0.1	19.9 ± 0.1	19.0 ± 0.1	18.4 ± 0.1	17.3 ± 0.1
200	8.72 ± 0.01	7.86 ± 0.045	7.26 ± 0.02	6.70 ± 0.03	6.26 ± 0.04	5.88 ± 0.05
205	3.31 ± 0.01	2.86 ± 0.01	2.50 ± 0.03	2.29 ± 0.02	2.12 ± 0.02	1.91 ± 0.02
210	1.21 ± 0.003	0.991 ± 0.003	0.835 ± 0.006	0.757 ± 0.006	0.655 ± 0.083	0.555 ± 0.002
215	0.440 ± 0.002	0.345 ± 0.001	0.276 ± 0.001	0.246 ± 0.006	0.197 ± 0.001	0.168 ± 0.001
220	0.162 ± 0.002	0.118 ± 0.0004	0.0926 ± 0.0003	0.0786 ± 0.0013	0.0626 ± 0.0003	0.0534 ± 0.0014
225	0.0600 ± 0.001	0.0409 ± 0.0006	0.0307 ± 0.0002	0.0253 ± 0.0002	0.0204 ± 0.0004	0.0176 ± 0.0046
230		0.0147 ± 0.0004	0.0110 ± 0.0002			
235		0.00553 ± 0.00025				

370 \* Quoted uncertainties are 2σ fit precision values (rounded off).

371

372



373

374 **Table 3.** Parameterization of the UV absorption spectra for CCl<sub>2</sub>FCCl<sub>2</sub>F (CFC-112), CCl<sub>3</sub>CClF<sub>2</sub>  
 375 (CFC-112a), CCl<sub>3</sub>CF<sub>3</sub> (CFC-113a), and CCl<sub>2</sub>FCF<sub>3</sub> (CFC-114a) obtained in this work. The  
 376 parameterization is for wavelengths between 192.5 to 235 nm and temperatures between 230 and  
 377 323 K for CFC-112 and CFC-112a and between 207 and 323 K for CFC-113a and CFC-114a.  
 378 Units:  $\sigma(\lambda, T)$  (cm<sup>2</sup> molecule<sup>-1</sup>, base e),  $\lambda$  (nm), and T (K)

$$\ln(\sigma(\lambda, T)) = \sum_i A_i \lambda_i^i + (T - 296) \sum_i B_i \lambda_i^i$$

Molecule	<i>i</i>	<i>A<sub>i</sub></i>	<i>B<sub>i</sub></i>
CCl <sub>2</sub> FCCl <sub>2</sub> F (CFC-112)	0	-1488.6207	6.04688
	1	18.43604	-0.0801501
	2	-0.02897393	0.0001201698
	3	-0.00051504703	2.610366 × 10 <sup>-6</sup>
	4	2.644261 × 10 <sup>-6</sup>	-1.3959106 × 10 <sup>-8</sup>
	5	-3.7258313 × 10 <sup>-9</sup>	2.0719264 × 10 <sup>-11</sup>
CCl <sub>3</sub> CClF <sub>2</sub> (CFC-112a)	0	-560.3404	10.37492
	1	9.534427	-0.182485408
	2	-0.06987945	0.0011614979
	3	0.0002657157	-2.9864183 × 10 <sup>-6</sup>
	4	-5.491224 × 10 <sup>-7</sup>	1.547878 × 10 <sup>-9</sup>
	5	4.993769 × 10 <sup>-10</sup>	3.36518 × 10 <sup>-12</sup>
CCl <sub>3</sub> CF <sub>3</sub> (CFC-113a)	0	-319.173	2.89174
	1	2.70954	-0.0348043
	2	0.00457404	3.6233 × 10 <sup>-5</sup>
	3	-0.0001288147	1.08853 × 10 <sup>-6</sup>
	4	4.71409 × 10 <sup>-7</sup>	-5.25744 × 10 <sup>-9</sup>
	5	-5.35388 × 10 <sup>-10</sup>	7.26095 × 10 <sup>-12</sup>
CCl <sub>2</sub> FCF <sub>3</sub> (CFC-114a)	0	-253.6338	0.52031
	1	2.899454	-0.005044
	2	-0.0081158	1.6142 × 10 <sup>-6</sup>
	3	-3.68328 × 10 <sup>-5</sup>	7.2259 × 10 <sup>-8</sup>
	4	2.071842 × 10 <sup>-7</sup>	2.4996 × 10 <sup>-11</sup>
	5	-2.5764 × 10 <sup>-10</sup>	-5.9642 × 10 <sup>-13</sup>

379

380



381

382 **Table 4.** Fractional losses and ranges (in parenthesis) for  $\text{CCl}_2\text{FCCl}_2\text{F}$  (CFC-112),  $\text{CCl}_3\text{CClF}_2$   
 383 (CFC-112a),  $\text{CCl}_3\text{CF}_3$  (CFC-113a), and  $\text{CCl}_2\text{FCF}_3$  (CFC-114a) calculated using the GSFC 2-D  
 384 model and the UV absorption spectra and estimated Lyman- $\alpha$  cross sections reported in this  
 385 work

Molecule	Lyman- $\alpha$	190-230 nm	$\text{O}(^1\text{D})$
$\text{CCl}_2\text{FCCl}_2\text{F}$ (CFC-112)	<0.001	0.978 (0.953–0.99)	0.022 (0.047–0.01)
$\text{CCl}_3\text{CClF}_2$ (CFC-112a)	<0.001	0.979 (0.955–0.99)	0.021 (0.045–0.01)
$\text{CCl}_3\text{CF}_3$ (CFC-113a)	<0.001	0.979 (0.968–0.986)	0.021 (0.032–0.014)
$\text{CCl}_2\text{FCF}_3$ (CFC-114a)	<0.001	0.929 (0.903–0.948)	0.071 (0.097–0.052)

386

387

388

389



390

391 **Table 5.** Atmospheric lifetimes ( $\tau$ )<sup>a</sup> and ranges<sup>b</sup> (years) for CCl<sub>2</sub>FCCl<sub>2</sub>F (CFC-112), CCl<sub>3</sub>CClF<sub>2</sub>  
 392 (CFC-112a), CCl<sub>3</sub>CF<sub>3</sub> (CFC-113a), and CCl<sub>2</sub>FCF<sub>3</sub> (CFC-114a) calculated using the GSFC 2-D  
 393 model and the UV absorption spectra reported in this work

Molecule	Tropospheric		Stratospheric		Mesospheric	Total	
	$\tau$	$\tau$ Range	$\tau$	$\tau$ Range	$\tau$	$\tau$	$\tau$ Range
CCl <sub>2</sub> FCCl <sub>2</sub> F (CFC-112)	2276	(1718–2710)	65.4	(64.2–66.3)	>10 <sup>6</sup>	63.6	(61.9–64.7)
CCl <sub>3</sub> CClF <sub>2</sub> (CFC-112a)	1187	(938–1371)	53.8	(52.8–54.6)	>10 <sup>6</sup>	51.5	(50.0–52.6)
CCl <sub>3</sub> CF <sub>3</sub> (CFC-113a)	1476	(1290–1645)	57.5	(56.7–58.3)	>10 <sup>6</sup>	55.4	(54.3–56.3)
CCl <sub>2</sub> FCF <sub>3</sub> (CFC-114a)	8312	(6286–10480)	106.7	(104.7–108.6)	3 × 10 <sup>5</sup>	105.3	(102.9–107.4)

394 <sup>a</sup> Global annually averaged values; <sup>b</sup> Calculated using 2 $\sigma$  upper and lower limits of the UV  
 395 absorption cross sections and estimated Lyman- $\alpha$  cross sections reported in this work (see text)  
 396 and O(<sup>1</sup>D) rate coefficient uncertainties from Sander et al. (2011).

397

398



399

400

401

**Table 6.** Lifetimes, ozone depletion potentials (ODPs), radiative efficiencies (RE), and global warming potentials (GWPs) obtained in this work and literature values for comparison

Molecule	Lifetime (years)	Ozone Depletion Potential (ODP)		Radiative Efficiency ( $\text{W m}^{-2} \text{ppb}^{-1}$ )	Global Warming Potential Time Horizons (years)		
		semi-empirical	2-D Model <sup>d</sup>		20	100	500
$\text{CCl}_2\text{FCCl}_2\text{F}$ (CFC-112)	63.6	0.88 (0.62-1.44) <sup>a</sup>	0.98 ( $\pm 0.015$ )	0.28	5330	4260	1530
$\text{CCl}_2\text{CClF}_2$ (CFC-112a)	51.5	0.88 (0.50-2.19) <sup>a</sup>	0.86 ( $\pm 0.015$ )	0.25	4600	3330	1110
$\text{CCl}_2\text{CF}_3$ (CFC-113a)	55.4	0.68 (0.34-3.79) <sup>a</sup>	0.73 ( $\pm 0.01$ )	0.24	4860	3650	1240
$\text{CCl}_2\text{FCF}_3$ (CFC-114a)	105.3		0.72 ( $\pm 0.01$ )	0.28	6750	6510	3000
$\text{CCl}_2\text{FCClF}_2$ (CFC-113)	93 <sup>b</sup>	0.81-0.82 <sup>b</sup>	0.95	0.30 <sup>b</sup>	6490 <sup>b</sup>	5820 <sup>b</sup>	
$\text{CClF}_2\text{CClF}_2$ (CFC-114)	189 <sup>b</sup>	0.50 <sup>b</sup>	0.78	0.31 <sup>b</sup>	7710 <sup>b</sup>	8590 <sup>b</sup>	
$\text{CClF}_2\text{CF}_3$ (CFC-115)	540 <sup>b</sup>	0.26 <sup>b</sup>	0.44	0.20 <sup>b</sup>	5860 <sup>b</sup>	7670 <sup>b</sup>	
$\text{CCl}_2\text{F}_2$ (CFC-12)	102 <sup>b</sup>	0.73-0.81 <sup>b</sup>	1.01	0.32 <sup>b</sup>	10800 <sup>b</sup>	10200 <sup>b</sup>	
$\text{CCl}_4$	26 <sup>b,c</sup>	0.72 <sup>b</sup>	1.06	0.17 <sup>b</sup>	3480 <sup>b</sup>	1730 <sup>b</sup>	

402 <sup>a</sup> Semi-empirical ODPs and uncertainty ranges taken from Laube et al. (2014).

403 <sup>b</sup> Taken from WMO (2014).

404 <sup>c</sup>  $\text{CCl}_4$  stratospheric lifetime of 44 years given in WMO (2014).

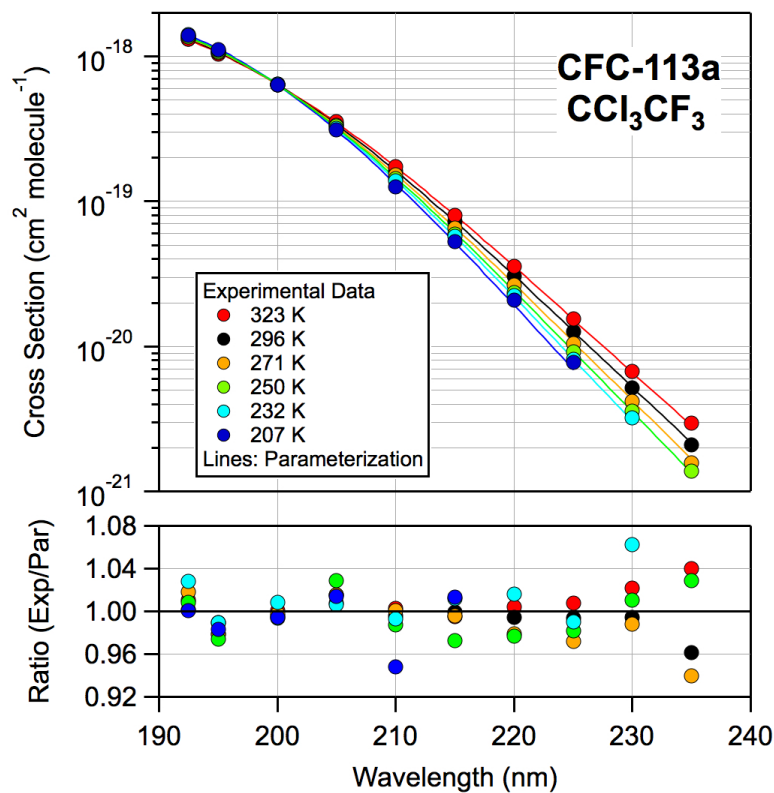
405 <sup>d</sup> The uncertainty range in the model calculated ODPs is due solely to the uncertainty in the UV  
 406 and Lyman- $\alpha$  (estimated) spectra obtained in this work and uncertainty in the  $\text{O}(^1\text{D})$  rate  
 407 coefficients taken from Sander et al. (2011).

408

409



410



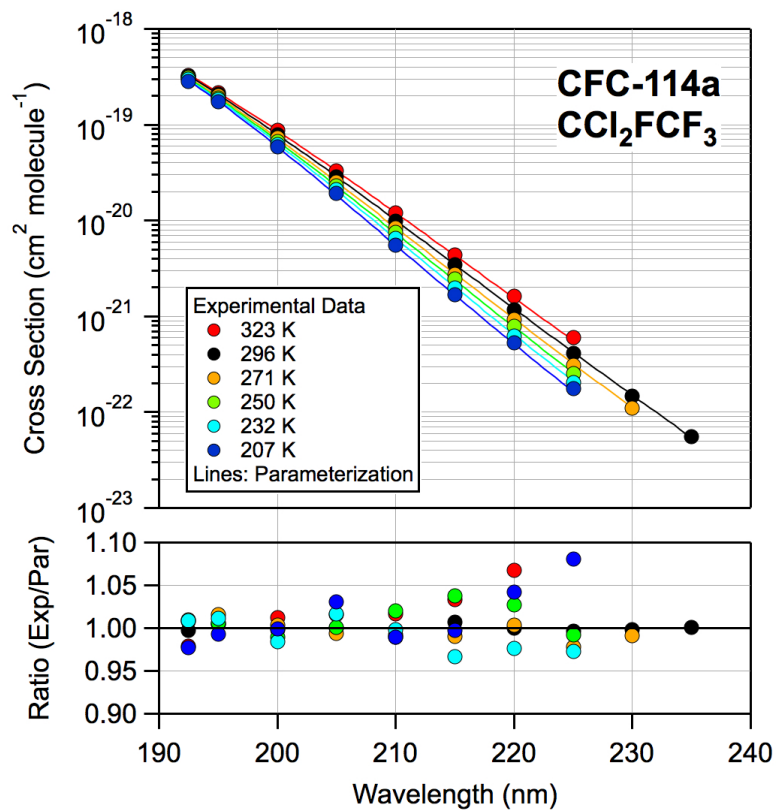
411

412 **Figure 1.**  $\text{CCl}_3\text{CF}_3$  (CFC-113a) UV absorption spectrum (base e) and parameterization obtained  
413 in this work. Cross section data (symbols, Table 1) and the parameterization of the data using  
414 the empirical formula and parameters given in Table 3 (see text). The lower frame shows the  
415 overall quality of the parameterization.

416



417  
418



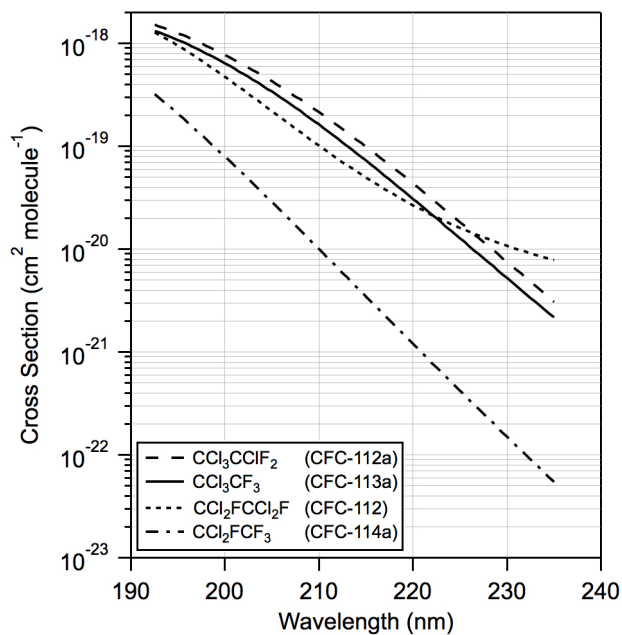
419  
420  
421  
422  
423  
424  
425  
426

**Figure 2.**  $\text{CCl}_2\text{FCF}_3$  (CFC-114a) UV absorption spectrum (base e) and parameterization obtained in this work. Cross section data (symbols, Table 2) and the parameterization of the data using the empirical formula and parameters given in Table 3 (see text). The lower frame shows the overall quality of the parameterization.



427

428



429

430 **Figure 3.** UV absorption spectra (base e) of CFC-112, CFC-112a, CFC-113a, and CFC-114a at  
 431 296 K calculated using the parameterization from this work, Table 3, over the wavelength range  
 432 of our experimental measurements.

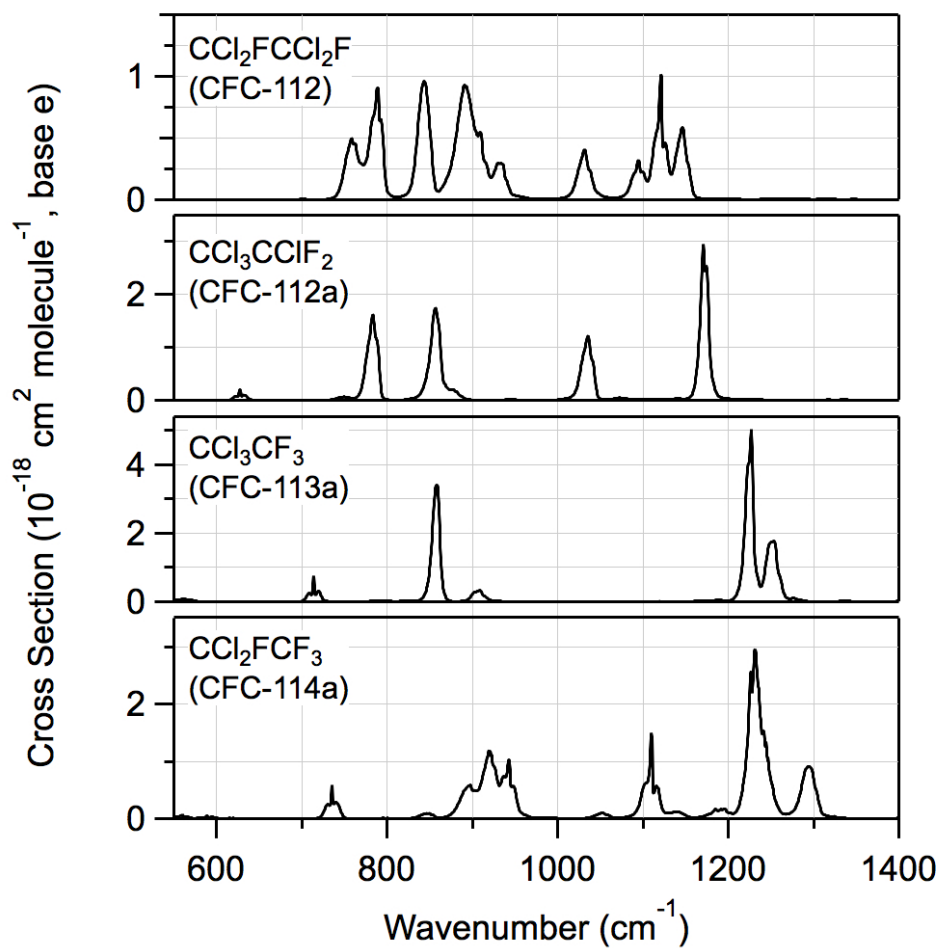
433

434



435

436



437

438

439 **Figure 4.** Infrared absorption spectra of  $\text{CCl}_2\text{FCCl}_2\text{F}$  (CFC-112),  $\text{CCl}_3\text{CClF}_2$  (CFC-112a),440  $\text{CCl}_3\text{CF}_3$  (CFC-113a), and  $\text{CCl}_2\text{FCF}_3$  (CFC-114a) at 296 K obtained in this work.

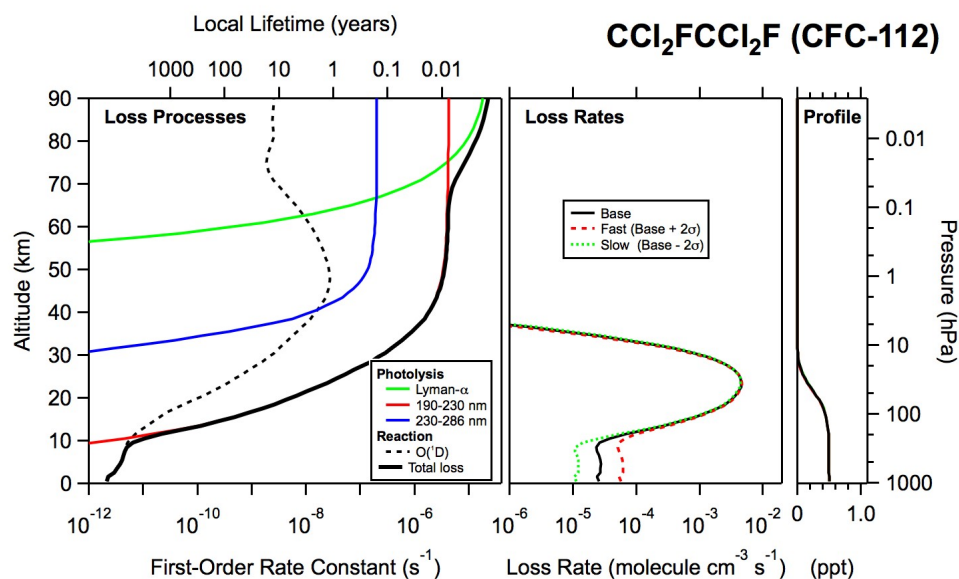
441

442

443



444  
445



446  
447  
448  
449  
450  
451  
452  
453  
454  
455

**Figure 5.** Global annually averaged vertical profiles of the atmospheric loss processes, molecular loss rates, and mixing ratio for  $\text{CCl}_2\text{FCCl}_2\text{F}$  (CFC-112) calculated using the GSFC 2-D atmospheric model for year 2000. The model calculations were performed using the CFC-112 UV absorption spectrum from this work and other model input parameters taken from the literature as described in the text. The global annually averaged lifetime for CFC-112 was calculated to be 63.6 (61.9–64.7) years.